MALAYSIAN JOURNAL OF APPLIED SCIENCES 2021, VOL 6 (2): 69-84
E-ISSN:0127-9246 (ONLINE)
https://doi.org/10.37231/myjas.2021.6.1.282
https://journal.unisza.edu.my/myjas

ORIGINAL ARTICLE

Optimization of Lead Base Perovskite Solar Cell with ZnO and CuI as Electron Transport Material and Hole Transport Material Using SCAPS-1D

**** Owolabi Joshua Adeyemi[1], Haruna Ali[1], Ismaila Musa[1], Ugbe Raphael Ushiekpan[1], Bamikole Johnson Akinade[2], Mohammad Lamido Madugu[3]***

[1]Department of Physics Nigerian Defence Academy, Kaduna, Nigeria
[2]Department of Physics, Federal University Lafia, Lafia, Nigeria
[3]Department of Physics, Faculty of Science, Gombe state University, Nigeria

[*]Corresponding author: owolabiy26@gmail.com

Received: 05/05/2021, Accepted: 30/10/2021, Published: 31/10/2021

Abstract

Perovskite solar cells (PSCs) research is substantially drawing attention because of the fast improvement in their power conversion efficiency (PCE), cheapness, possibility to tune the bandgap, low recombination rate, high open circuit voltage, excellent ambipolar charge carrier transport and strong and broad optical absorption. In this research, Zinc oxide as electron transport material (ETM) and copper iodide as hole transport material (HTM) have been optimized using SCAPS-1D simulation software. The thickness, bandgap, of ZnO (ETM) and CuI (HTM) was investigated. Results shows that the thickness and bandgap were found to strongly influence the PCE of perovskite solar cell. ZnO/CuI was found to be a better replacement to TiO2/Cu2O for stability and low degradation rate. It was observed that the maximum efficiency is 22.04%, Voc of 0.84V, JSC of 32.83mA/cm2 and FF of 79.79% was obtained when the thickness of ETM and HTM layer of (CH3NH3PbI3) PSCs which was found to be optimum at 0.2μm for the final optimization.

Keywords: Perovskite solar cells (PSCs), ZnO, ETM, CuI, HTM, SCAPS-1D

Introduction

Various promising solar cell concepts, ranging from single-crystal silicon to thin-film materials to solely organic cells, have been widely developed and demonstrated over the last few decades. In view of the current state of the art of large-scale solar cell fabrication, expense, efficiency, durability and potential must be taken into account. A recent and exciting approach for cost-effective, durable and scalable PV technology is the use of solution-processed earth-rich inorganic materials in the manufacture of solar cells. Organic-inorganic hybrid perovskites have received valuable interest as an absorber layer in thin film solar cells since the invention of methylammonium lead halide based solar cells (Kojima, 2006). The features displayed by these

materials are ideal for low-cost photovoltaic (PV) applications, such as high absorption coefficients, excellent transport properties, tunable bandgap, lack of deep trap states within the bandgap, low-temperature processing, etc. In a comparatively short time, the photo-conversion performance of perovskite solar cells has significantly increased from 3.8% to 19.1%. The above-mentioned lead halide perovskite material characteristics promote it use in the manufacture of perovskite solar cells and make it a good competing material for the conventional silicon material. The maximum PCE of these perovskite solar cells based on CH3NH3PbI3 has previously been 3.8 percent (Kojima, 2006 and Lingyan et al., 2019). In due course, the PCE of perovskite solar cells will be improved by the new fabrication methods and the right selection of device architecture.

In this research, we propose to optimize theHTM (CuI) andETM (ZnO) of lead base Perovskite solar cells (PSCs) with fluorine doped tin oxide (FTO) as transparent conducting oxide (TCO) using solar cell capacitance simulation software – one Dimension (SCAPS -1D).Compared to their counterparts, it is notable that tin-based perovskite has so far demonstrated poorer system efficiency and is much more vulnerable to degradation as a result of self-oxidation and high instability (Noel et al., 2020). Tin cannot be a suitable lead surrogate in order to preserve stability and high PCE in lead-based perovskite solar cells, but a greater reduction in the toxicity of lead can be used, such as full encapsulation methods against moisture and oxygen ingress and the use of low lead-based perovskite (Yifan et al., 2019) Computer simulation is a helpful technique that can provide useful knowledge for the material screening phase to be experimentally evaluated, solar cell capacitance simulation software (SCAPS) is affordable, saves time and resources; it has a range of solar cell-related properties such as concentration of energy bands, I-V characteristics, C-V, C-F and QE and also has a very intuitive operating window.

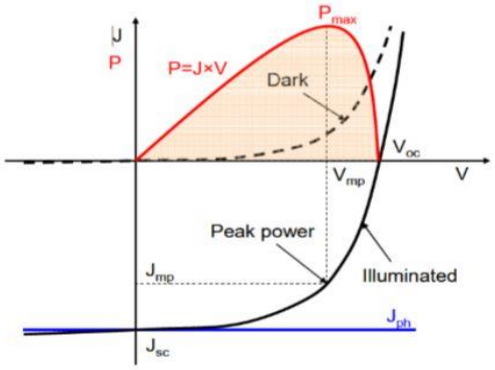

Figure 1: *J -V characteristics of a p-n junction in the dark and under illumination*

Modeling and Simulation of Device

Computational simulation is a process by which the behavior of a real device or theoretical model is observed and evaluated by mimicking it with a computer application. Simulation is based on a system-describing mathematical model. Over the years, numerical simulation methodology of solar cell devices has proved to be a viable instrument for the study and interpretation of solar cell system properties, such as the structural, electrical and mechanical properties of complex solar cell devices. It also aims to minimize the cost of processing and time spent on producing solar cell devices by providing valuable knowledge on how the production parameters can be varied to enhance the efficiency of the cell. (Minemoto et al., 2014).

The main parameters that are used to characterize the performance of solar cells are the peak power, P_{max}, the short-circuit current density, J_{SC}, the open-circuit voltage, V_{OC} and the Fill

Factor, FF. These parameters are determined from the J -V illuminated characteristic curve as illustrated in Figure 1. The conversion efficiency, η is determined from these parameters.

The photovoltaic parameters used to describe the performance of a photovoltaic device are short circuit current density (J_{SC}), open circuit voltage (V_{OC}), fill factor (FF) and conversion efficiency (η). SCAPS-1D is one-dimensional simulation software developed by Burgelman et al. from the University of Gent, Belgium. SCAPS can be determined by variety of properties related with solar cells such as energy bands, concentrations, currents, I-V characteristics, C-V, C-f, and QE. The flow chart below shows procedures in running a simulation with SCAPS and its action panel are shown in figure 2.

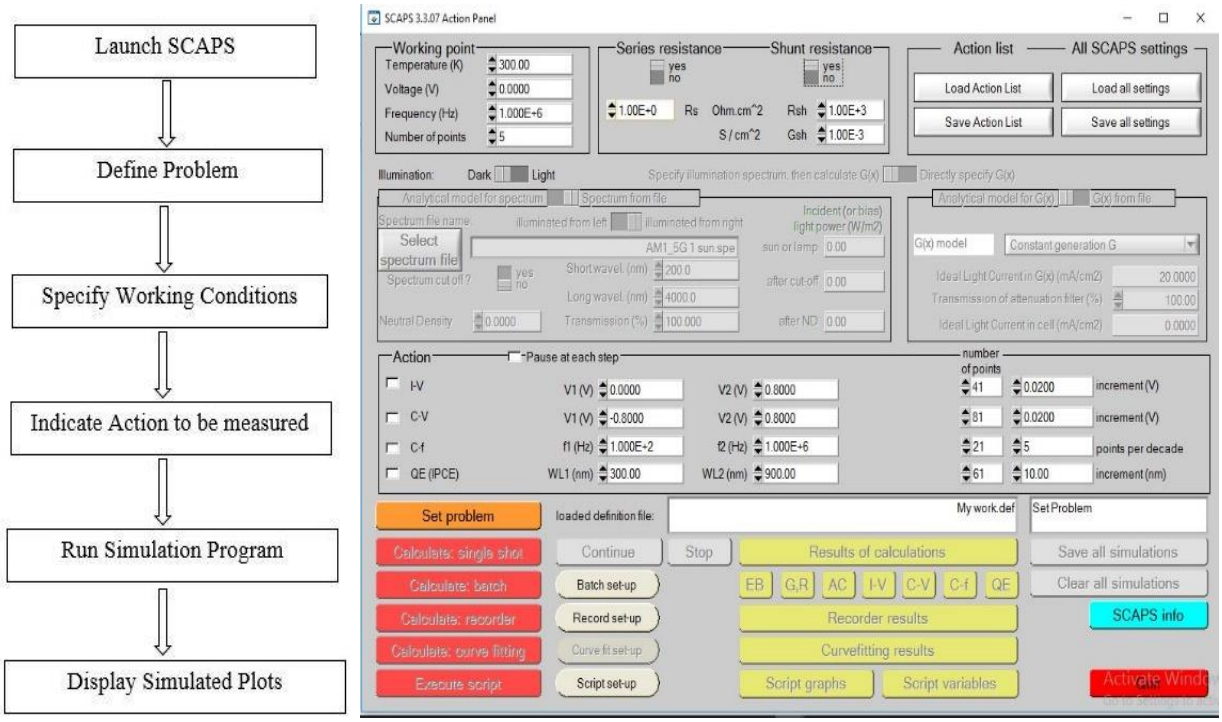

Figure 2: SCAP flow chart and working interface

Shows the working procedures of SCAPS to define the problem starting with the launch of the program on the computer; here you set layers and the nature of the solar cell you want to model and set the working conditions of the scanning voltage, temperature, and absorption range. Then define the parameter to calculate the spectrum from I-V, C-V, and QE, when all these conditions set its time for the simulation to run and display the simulated outcome for further analysis.

Fabrication of perovskites solar cell is achieved in two planar sructures p-i-n and n-i-p the latter are the most commonly used which comprises of TCO/ETL/perovskite/HTL/metal structure, where TCO, ETL and HTL refer to transparent conducting oxide, electron transport layer, hole transport layer respectively and the perovskite material (absorber layer) is the independent layer of the solar cell. The cell model is based on FTO/ZnO/$CH_3NH_3SnI_3$/CuI/Ag and the energy bandgap used for this simulation is shown in Figure 3.

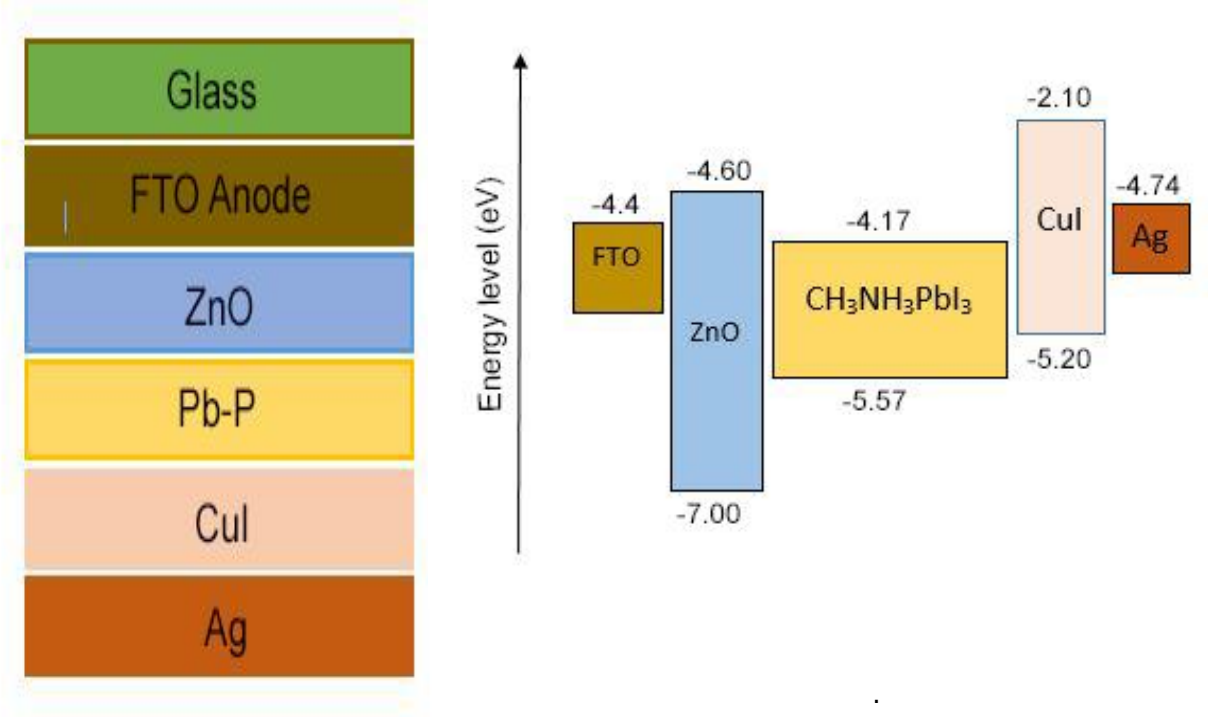

Figure 3: Device structure and energy band diagram of ETM, HTM with absorber layer

Figure 3 shows the material layers and the energy band diagram of the device respectively. Light enters the cell through the transparent conductive oxide layer (FTO), passes through the compact electron transporting layer (ZnO), the defect layer ZnO/$CH_3NH_3PbI_3$ which is partly an absorber and enters the absorber which also has an interface defect $CH_3NH_3PbI_3$/CuI to the hole transport material (CuI) and the energy level of the simulation architecture, the highest occupied molecular orbital (HUMO) of CuI is above the valence band (VB) of the absorber layer and the lowest unoccupied molecular orbital is also above the conduction band (CB) of the absorber layer to prevent electron transport to the back contact electrode gold (Au). The HTM (CuI) also prevent the infiltration of the gold electrode into the absorber layer.

Figure 4 shows the model of sandwiched simulation structure, the toxicity nature of lead based absorber, which is water-soluble, makes it more source of concern. This can be mitigate this simulation structure as copper iodide (CuI) and zinc oxide (ZnO) are both hydrophobic in nature there by shielding the absorber layer from moisture.

The parameters for different layers in the simulation are chosen on the basis of theoretical considerations, experimental data and existing literature or in some cases, reasonable estimation (Lingyan et al, 2019 and Salah et al, 2018) Thermal velocities of the electron and hole are both set to be equal to 107 cm/s but for the perovskite layer are set to be 106 cm/s. The absorber is a p-type semiconductor doped with a carrier density of 3·2x1015 cm–3.

The defects in the absorption layer are set to be neutral, Gaussian energetic distribution with a characteristic energy of 0.1eV, with a defect density of 1016 cm–3 but absorber layer is 1014 cm–3. The work function of FTO and metal back contact for hole transport are considered to be 4.40eV and 4.74eV (Salah et al., 2018) respectively. All the simulations operate under the

scanning voltage from 0V to 1.2V. All simulations in this work were performed under ambient temperature (300 K). The electrical parameters are VOC, JSC, FF and efficiency generated by SCAPS-1D were then used to determine the optimum thickness, bandgap of the ETM and HTM layers in the configuration. The current density voltage (J-V) curves of the optimized solar cells from the simulation were then determined.

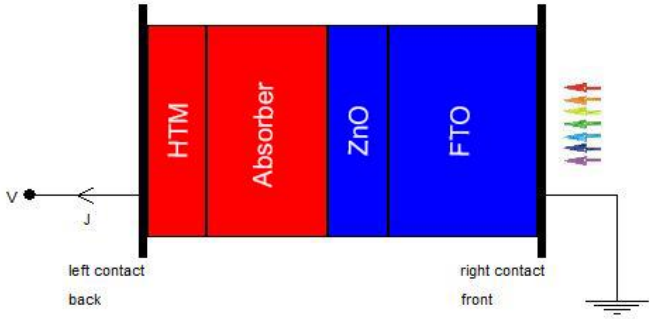

Figure 4: Model of sandwiched simulation structure

Results and Discussions

Effect of ZnO as ETL and CuI as HTL on the J-V Curves of PSC

Figure 5 shows simulated J-V curves for a $CH_3NH_3PbI_3$ based device in the planar electron-absorber-hole (n-i-p) configuration with ZnO as ETL and CuI as HTLwith the output cell parameters Voc = 0.76V, Jsc = 32.85mA/cm^2, FF = 71.74%, and PCE(η) = 17.94% under AM1.5 simulated sunlights of 100mW/cm^2.

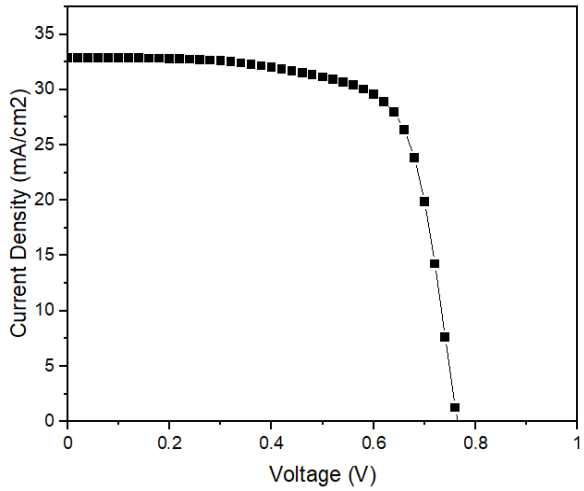

Figure 5: *J-V curve of the photovoltaic structure with initial parameters*

Effect of thickness of ETL (ZnO)

The effect of the thickness on zinc oxide (ETL) on the performance parameters of the cell ranging from 1.60μm to 0.80μm was obtained in Figure 6. Table 1 shows that when there is an increase in the thickness of electron transporting material it results in a decrease in J_{SC}, FF and efficiency of the device while V_{OC} decreases but remain invariable from 0.84V at the thickness of 1.60μm.

Varying the thickness of ETL signifies that when the material is thicker, it provides a longer diffusion path for the electron to reach the electrode which limit (the solar cell parameters) the charge collection efficiency and transmitting of an incident photon decreases with increasing thickness. High performance was obtained, when the thickness of ETL is 0.20μm with J_{SC} of 32.84mA/cm^2, V_{OC} of 0.84V, FF of 79.70% and high PCE of 22.87%.

Table1: Dependence of solar cell performance on thickness of ZnO (ETL)

ZnO thickness (μm)	J_{SC} (mA/cm^2)	V_{OC} (V)	FF (%)	PCE (%)
1.60	32.84	0.84	79.70	21.24
1.40	32.84	0.84	79.70	21.53
1.20	32.84	0.84	79.70	22.74
0.20	32.83	0.84	79.70	22.87
0.40	32.83	0.84	79.70	22.04
0.60	32.83	0.84	79.70	21.84
0.80	32.83	0.84	79.70	22.15

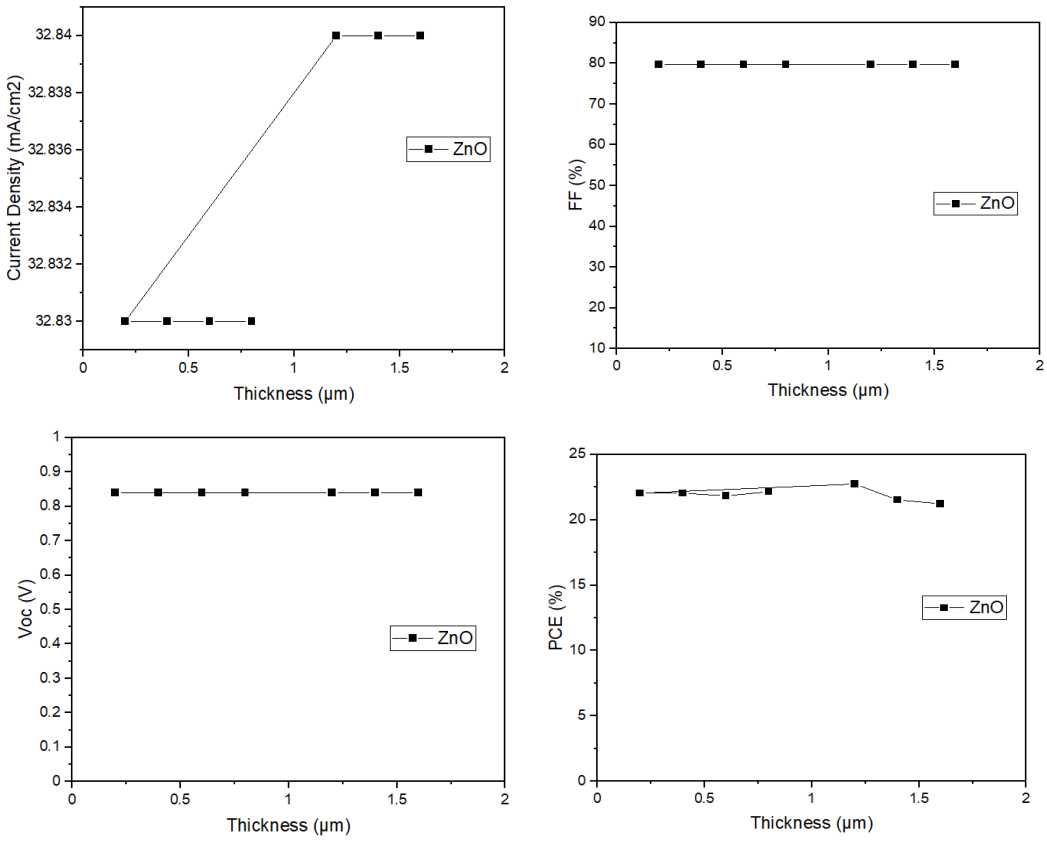

Figure 6: *Variation in performance parameters of PSC with thickness of ZnO (ETL)*

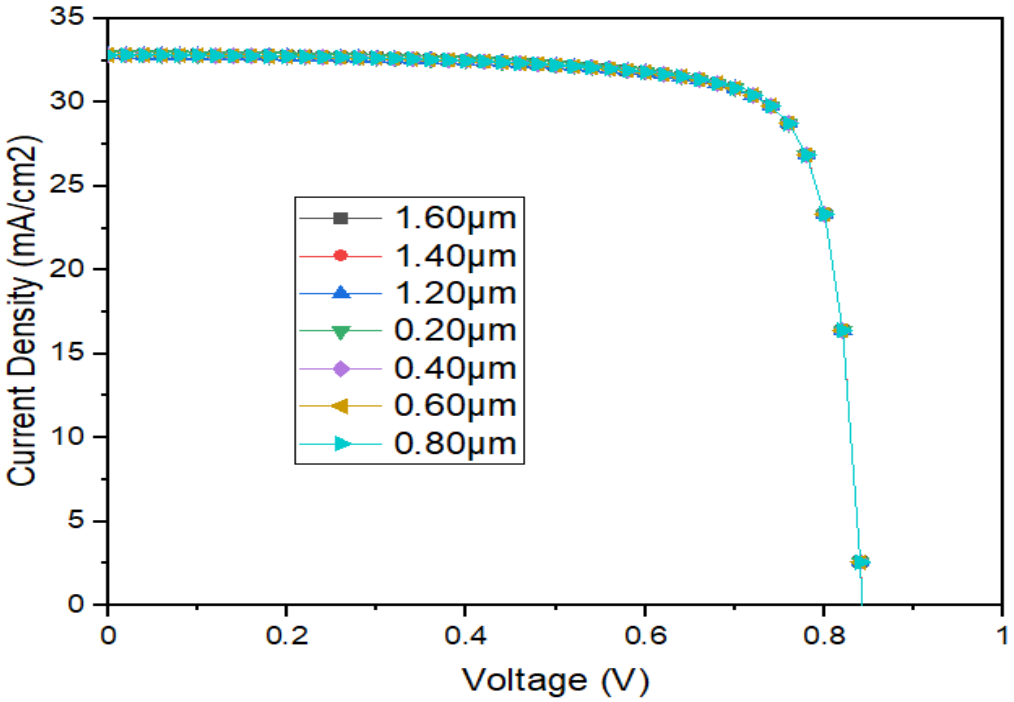

Figure 7: *J-V curves of PSC with different values of ZnO (ETL) thickness*

Effect of thickness of HTL (CuI)

The variation of the whole transport layer (HTL) It was observed that the increase in thickness of the HTM improves the performance of the solar cells due to increase in recombination and resistance of the device.

The effect of the thickness on copper iodide (HTL) on the performance parameters of the cell ranging from 1.60µm to 0.80µm was obtained in figure 8. Table 2 shows that when there is an increase in the thickness of electron transporting material it results in a decrease in J_{SC}, FF and efficiency of the device while V_{OC} decreases but remain invariable from 0.84V at the thickness of 1.60µm. Varying the thickness of HTM signifies that when the material is thicker, it provides a longer diffusion path for the hole to reach the cathode which limit (the solar cell parameters) the charge collection efficiency and transmitting of an incident photon decreases with increasing thickness. High performance was obtained, when the thickness of HTM is 0.20µm with J_{SC} of 32.84mA/cm^2, V_{OC} of 0.84V, FF of 79.70% and high PCE of 22.04%.

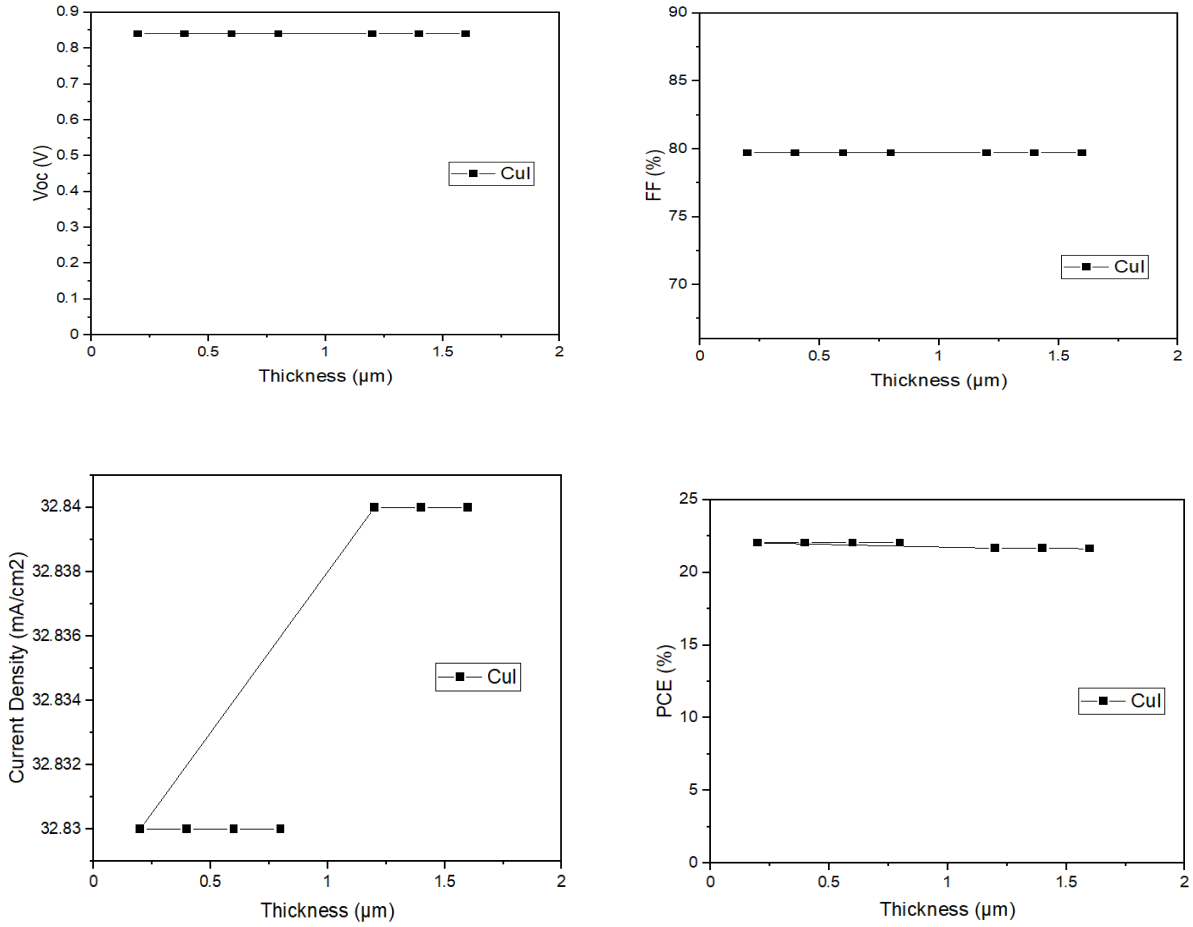

Figure 8: *Variation in performance parameters of PSC with thickness of CuI (HTL)*

Table 2: *Dependence of solar cell performance on thickness of CuI (HTL)*

CuI thickness (μm)	J_{SC} (mA/cm^2)	V_{OC} (V)	FF (%)	PCE (%)
1.60	32.84	0.84	79.70	21.64
1.40	32.84	0.84	79.70	21.66
1.20	32.84	0.84	79.70	21.66
0.20	32.83	0.84	79.70	22.04
0.40	32.83	0.84	79.70	22.04
0.60	32.83	0.84	79.70	22.04
0.80	32.83	0.84	79.70	22.04

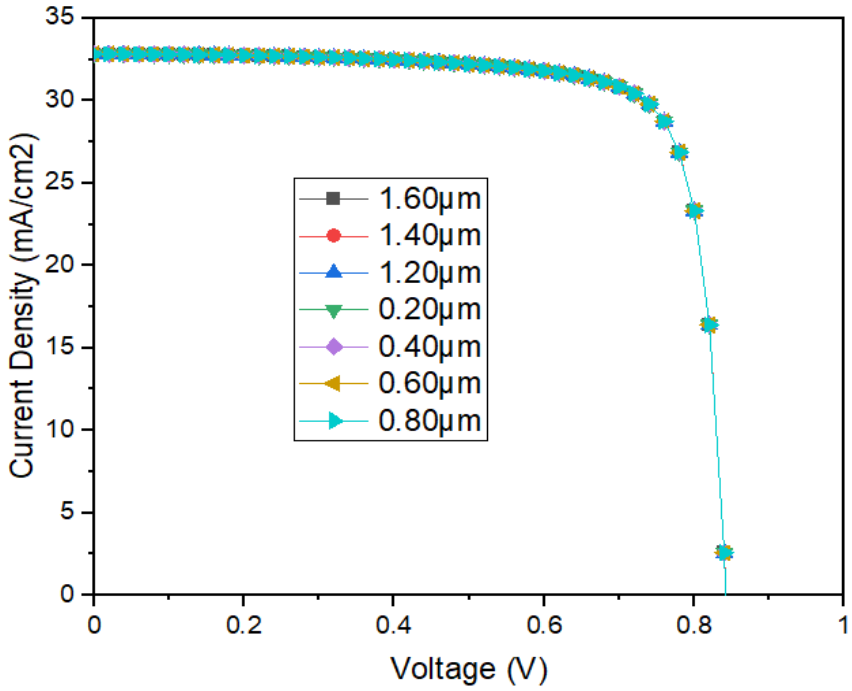

Figure 9: *J-V curves of PSC with different values of CuI (HTL) thickness*.

3.4 Effect of bandgap of ETL (ZnO)

The effect of bang of ETM layer is very important as it depends on the nature and properties of the material. ZnO has a wide direct bandgap, which makes favorable properties such as good transparency and relatively high electron mobility.

Table 3: *Dependence of solar cell performance on ZnO (ETM) bandgap*

ZnO bandgap (eV)	J_{SC} (mA/cm^2)	V_{OC} (V)	FF (%)	PCE (%)
2.30	28.32	0.83	79.91	18.99
3.80	32.79	0.84	79.69	22.02
4.20	32.83	0.84	79.69	22.03
4.40	32.83	0.84	79.69	22.04
5.20	32.83	0.84	79.69	22.04
6.40	32.83	0.84	79.69	22.04
6.80	32.83	0.84	79.69	22.04

In table.3, it was observed that when the bandgap was varied from 2.30eV to 6.80eV, it results to an increase in J_{SC} of 32.83mA/cm^2 at 4.20eV and PCE of 22.04%, at the same bandgap. FF of 79.69% and V_{OC} at 0.84V is stable (invariable) throughout without considering the reduction of light absorption because the quantity of Exciton generation is increased which in turn increases the efficiency of the solar cell.

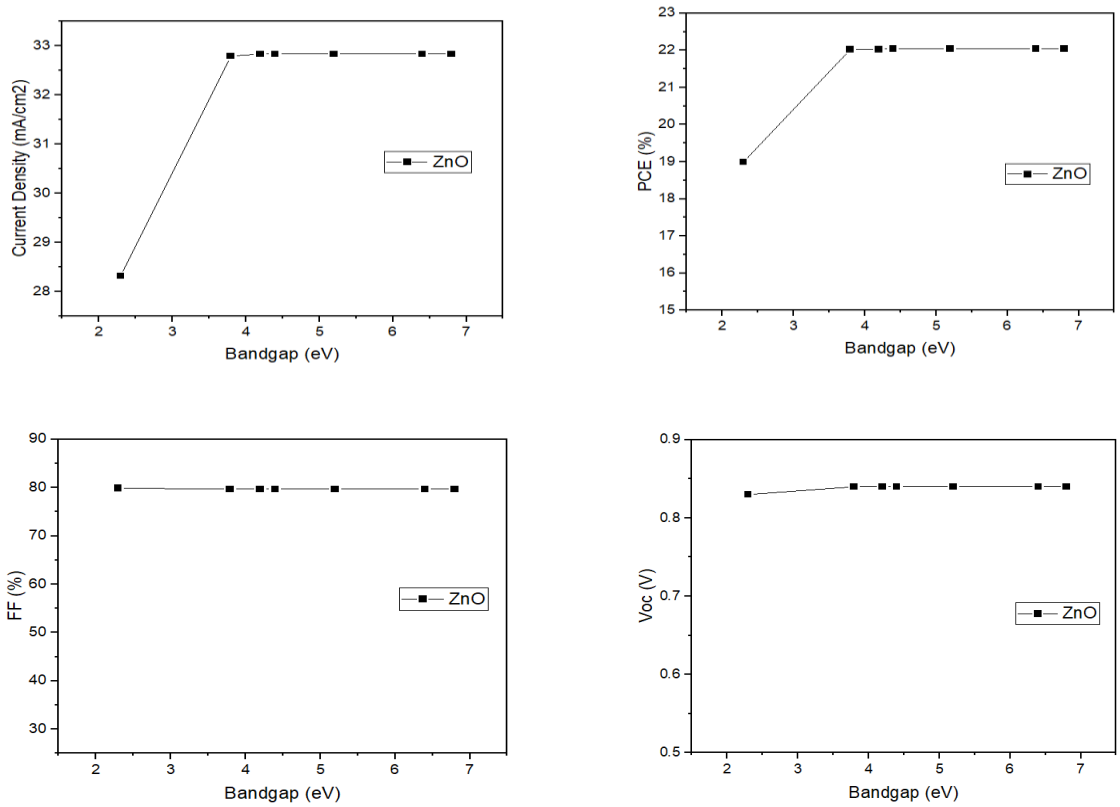

Figure 10: *Variation in performance parameters of PSC with bandgap of ZnO (ETM)*

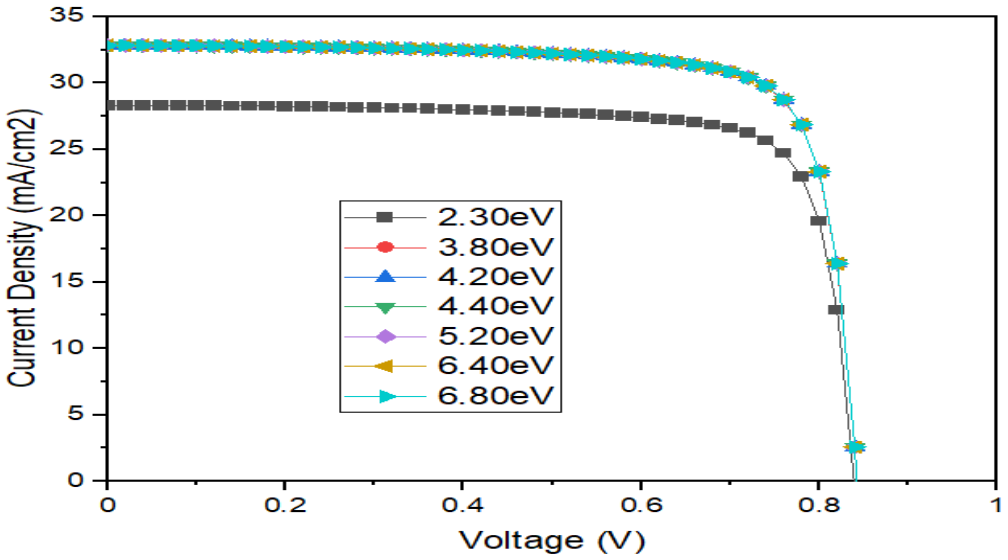

Figure 11: *J-V curves of PSC with different values of ZnO (ETM) bandgap*

Effect of bandgap of HTL (CuI)

Table 4 shows how the bandgap affects the open circuit voltage of the device it was found that at bandgap of 3.20eV and 3.60ev there was discontinuity as a result of the absence in the Voc and FF and shown in table 4 this was as a result of the bandgap not within the tunable bandgap of the material.

Table 4: Dependence of solar cell performance on CuI (HTM) bandgap

CuI bandgap (eV)	J_{SC} (mA/cm^2)	V_{OC} (V)	FF (%)	PCE (%)
2.00	31.21	0.27	53.74	4.53
2.40	32.22	0.47	64.22	9.80
2.60	32.83	0.84	79.69	22.05
3.10	32.86	0.84	82.61	22.93
3.20	32.88	-	-	3.29
3.40	32.88	0.85	86.63	24.18
3.60	32.83	0.38	-	12.04

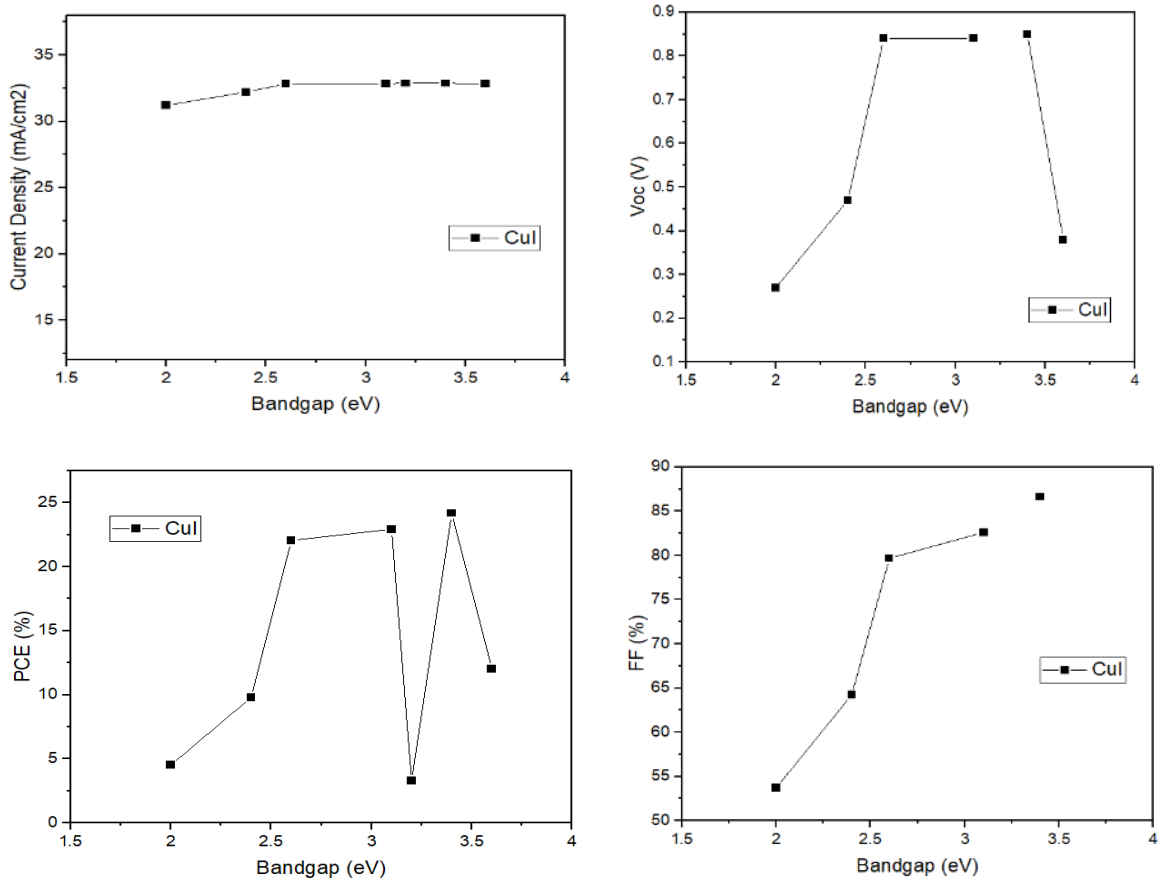

Figure 12: *Variation in performance parameters of PSC with bandgap of CuI (HTM)*

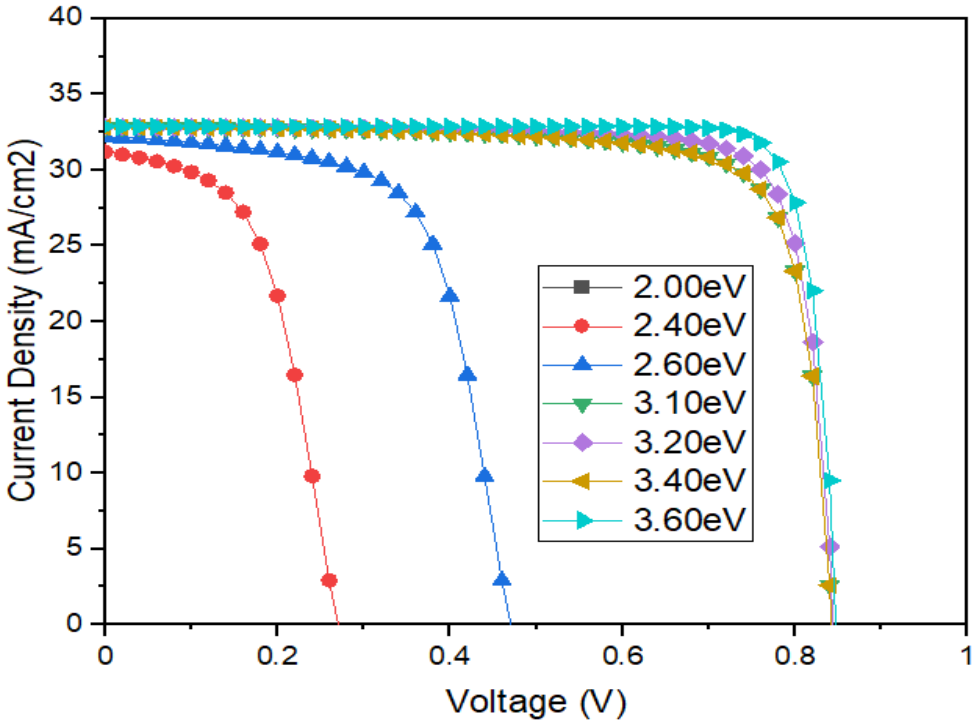

Figure 13: *J-V curves of PSC with different values of CuI (HTM) bandgap*

Performance of optimized parameters

The thickness, bandgap, were considered as the following factors by which we obtain J_{SC} of 32.83mA/cm^2, V_{OC} of 0.84V, FF of 79.69% and PCE of 22.04%. The final optimized parameters of perovskite solar cell in the simulation and optimized J-V curve are shown in Table 5, Figure 14 respectively. The simulated results were compared with the experimental work published by other researchers and the related data was summarized in Table 6.

Table 5. Optimized parameter of the device

Optimized Parameters	**ETM (ZnO)**	**HTM (CuI)**
Thickness (µm)	0.20	0.20
Bandgap, Eg (eV)	4.40	3.10
Donor density, (cm^3)	10^{20}	---
Acceptor density, (cm^{-3})	---	10^{20}

Figure 14 shows the J-V characteristics curve obtained by simulating with optimized parameters with output cell parameters Voc = 0.84V, Jsc = 32.83mA/cm2, FF = 79.69% and, PCE (η) = 22.04%.

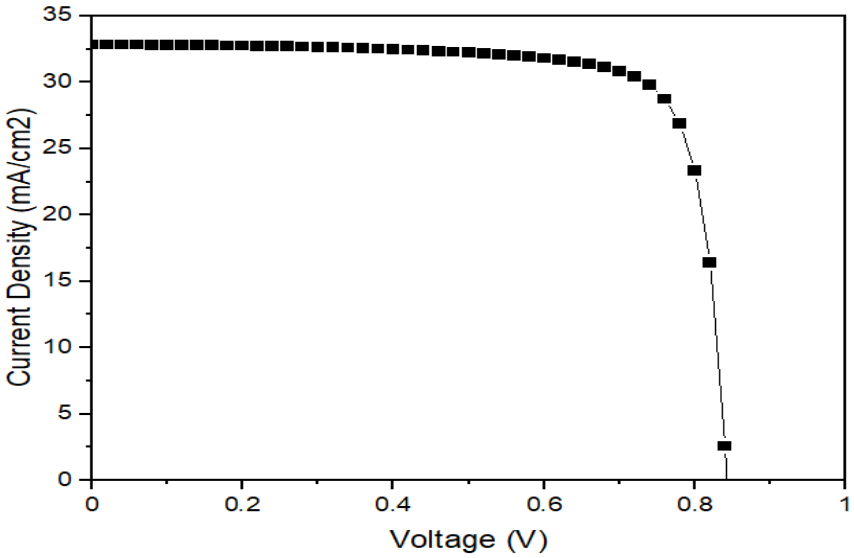

Figure 14: J-V curves analysis for PSC with optimized parameters

These values are similar to the simulation values from literature [34]. as Voc = 1.15V, Jsc = 21.55mA/cm2, FF = 87.51, η = 21.79%. This result confirms our new configuration as equivalent to the real device structure.

Table 6: Using SCAPS to report the photovoltaic parameters of copper iodide-based perovskite solar cells, experimental work in the literature and simulated results

Simulation	J_{SC} (mA/cm^2)	V_{OC} (V)	FF (%)	PCE (%)
Initial	32.85	0.74	71.74	17.94
Optimized Thickness of ETM	32.83	0.84	79.69	22.87
Optimized Thickness of HTM	32.84	0.84	79.69	22.04
Optimized Bandgap of ETM	32.97	0.84	67.72	22.04
Optimized Bandgap of HTM	32.86	0.84	82.61	22.93
Final Optimization	32.83	0.84	79.69	22.04
Experimental Parameters	18.67	0.68	47.43	6.09
Experimental Parameters	31.59	0.92	79.99	23.36

Conclusion

In conclusion, the purpose of this research study was to use SCAPS-1D to study lead-based ($CH_3NH_3PbI_3$) perovskite solar cell integration of copper iodide (CuI) as HTL with ZnO as ETL, and its effect on the electrical performance of the cell. it was discovered that lead-based perovskite solar cells with zinc oxide (ZnO) and copper iodide (CuI) as an electron transporting material (ETM) and hole transporting material (HTM) respectively can attain PCE of 22.04% with an optimum thickness value of 0.20μm for ETM and HTM respectively.In the simulation, the defect density in the absorber layer is the most critical factor for the high performance of a solar cell. By choosing the defect density as 1×10^{20} cm^{-3}. Other solar cell parameters such as bandgap, was also optimized to achieve the final power conversion efficiency (PCE) of 22.04%. The planar configuration in this simulation using SCAPS 1-D was found to be in accordance with experimental work from literature.

Acknowledgement

The authors thank Professor Marc Burgelman, Department of Electronics and Information Systems at the University of Gent for the development of SCAPS-1D and its free access.

References

Amu Tochukwu loreta (2014) performance optimization of tin halide perovskite solar cells via numerical Simulation.

Burgelman M., Koen D., Alex N., Johan V., and Stefaan D., (2014). “SCAPS manual”.

Chen Y, Peng J, Diqing S, Chen X, Liang Z. (2015) Efficient and balanced charge transport revealed in planar perovskite solar cells. *ACS Applied Materials and Interfaces, 7(*8), 4471–5.

D. Eli, M.Y Onimisi, S. Garba, A.O. Mohammed (2019) Simulation and optimization of lead – based Perovskite solar cell with Cu2O and TiO2 as p-type and n-type layer.

Dong Q, Fang Y, Shao Y, Mulligan P, Qiu J, Cao L, Huang J. (2015). Electron-hole diffusion lengths 175 mm in solution-grown CH3NH3 PbI3 single crystals*. Science, 347*(6225), 968–70.

Fan, J., Jia, B., & Gu, M. (2014). Perovskite-based low-cost and high-efficiency hybrid halide solar cells. *Photonics Research, 2*(5), 111-129.

Giannelis E. P (1996) “Polymer layered silicate nanocomposites,” Advanced Material, 8 (1),29–35.

Green. M. A., Keith E.,Yoshihiro H., Ewan D., (2013). “Solar cell efficiency tables (version 43),” pp. 1–9.

Green. M.A., Ho-Baillie.A., and Snaith .H.J., (2014). The emergence of perovskite solar cells. Nature Photonics, 8(7), nphoton-2014.

Guan-Syun Chen, Yi Ching Chen, Ching-Ting Lee, Hsin-Ying less (2018) Performance improvement of perovskite solar cells using electron and hole transport layers, Yuan Ze University, Taiwan Republic of China, Elsevier Ltd.

Hui-Jing Du, Wang W.C., and Zhu J.Z., (2016). “Device simulation of lead-free CH3NH3SnI3 perovskite solar cells with high efficiency,” Chinese Physics B, vol. 25

Hsiao YC, Wu T, Li M, Liu Q, Qin W, Hu B. (2015) Fundamental physics behind high-efficiency organo-metal-halide perovskite solar cells*. Journal of Material Chemistry A*., *3*(30),15372–15385.

Kazim S, Nazeeruddin MK, Grätzel M, Ahmad S. (2014) Perovskite as light harvester: A game changer in photovoltaic’s. Angewandte Chemie International Edition.

Khelifi S., Voroshazi E., Spoltore D., Piersimoni F., Bertho S., Aernouts T., Manca J., Lauwaert J., Vrielinck H., Burgelman M., (2014) “Effect of lighting induced degradation on electrical transport and charge extraction in polythiophene; fullerene (P3HT: PCBM) solar cells.

Kim J., (2014) “The role of intrinsic defects in methylammonium lead iodide perovskite”, *The Journal of Physical Chemistry Letters, 5*, 1312–1317.

Kojima A, Kenjiro T, Shirai Y, Miyasaka T. (2009) Organometal halide perovskites as visible-light sensitizers for photovoltaic cells. *Journal of American Chemical Society, 131*(17), 6050–6051.

Kojima A., “Novel (2006). photoelectrochemical cell with mesoscopic electrodes sensitized by lead-halide compounds (2). In Proc. 210th ECS Meeting.

Lingyan Lin, Linqin Juan, ping Li, Baodian Fan, you Qui, Fengpo Yan (2019). Simulation of optimum band structure of HTM free perovskite solar cells based on ZnO electron transporting layer: material science in semiconductor 90, 1-6.

Luo S, Daoud WA. (2015) Recent progress in organic-inorganic halide perovskite solar cells: Mechanisms and material design. *Journal of Material Chemistry A., 3*(17), 8992–9010.

Mandadapu, U., Vedanayakam, S.V., Thyagarajan, K. and Babu, B.J. (2018) ‘Optimisation of high-efficiency tin halide perovskite solar cells using SCAPS-1D’, *Int. J. Simulation and Process Modelling, 13(*3), 221–227.

McGraw-Hill (2002). Concise, Encyclopedia of Physics. The McGraw-Hill Companies, Inc,

Minemoto. T and M. Murata, (2014) “Device modeling of perovskite solar cells based on structural similarity with thin film inorganic semiconductor solar cells,” *J. Appl. Phys., 116*, 054505,

Minemoto T, and Murata M. (2014). Impact of work function of back contact of perovskite solar cells without hole transport material analyzed by device simulation. Curr. *Appl Phys; 14,*1428–1433.

Mola G T. (2015) Enhanced photon harvesting in OPV using an optically reflective surface. Applied Physics. *Materials Science and Processing, 118*(2), 425–29.

Mohammad I.Hossain, Fahhad H. Alharbi, Nouar tabet (2015) copper oxide as inorganic hole transport material for lead halide perovskite based solar cells.

M. Zeman (1999) Introduction to photovoltaic solar cell energy. Pp.1-139

Nelson. J (2003), The Physics of Solar Cells. Imperial College Press: London, pp. 1–325.

Noh J.H, (2013) “Chemical management for colorful, efficient, and stable inorganic-organic hybrid nanostructured solar cells" *Nanoletters, 13,* 1764−1769.

Sandeep K.P., Michael B.J., Annamaria P., Laura M.H., and HenryJ.S, (2014). “Lead Free Organic-Inorganic Tin Halide Perovskites for Photovoltaic applications,” *Energy Environ. Sci., 7,* 3061–3068.

NREL efficiency chart [Online]. Available: http://www.nrel.gov/ncpv/images/efficiency_chart.jpg

Park N.G., (2015) “Perovskite solar cells: An emerging photovoltaic technology” Mater. Today, 18, 65−72.

Rongsheng Wei (2108) modelling of perovskite solar cell. Queensland University of Technology.

Salah MM, Hassan KM, Abouelatta M, Shaker A, (2018), A Comparative Study of Different ETMs in Perovskite Solar Cell with Inorganic Copper Iodide as HTM, Optik https://doi.org/10.1016/j.ijleo.2018.10.052

Shubhra B., A. Puruswottan (2016), Evaluation of new materials for electron and Hole Transport Layer in Perovskite base solar cell through SCAPs- 1D simulation, University of Nevada Las Vegas N89052, USA, IEEE.

Stranks S. D., (2013) “Electron-hole diffusion lengths exceeding 1 micrometer in an organometal trihalide

perovskite absorber" *Science, 342,* 341−344,

Syed Zulqarnain Haider, Hafeez Anwar, Mingqing weng (2018). A Comprehensive device modeling of perovskite solar cell with inorganic copper iodide as Hole transport material.

Tan, K., Lin, P., Wang, G., Liu, Y., Xu, Z., Lin, Y., (2016) Controllable Design of Solid-State Perovskite Solar Cells by SCAPS Device Simulation, Solid-State Electronics, doi: http://dx.doi.org/10.1016/ j.sse.2016.09.012

Tessema G. (2012) Charge transport across the bulk-heterojunction organic thin film. Applied Physics. *Materials Science and Processing, 106*(1), 53–57.

V. Balema, "Alternative Energy Photovoltaics, Ionic Liquids, and MOFs," Mateial Matters, 4(4), 1-10.

Wayesh Q, Yesmin AJ, Gloria MD, Tashfiq M, Hossain MI, Islam SN. (2015) Optical analysis in $CH_3NH_3PbI_3$ and $CH_3NH_3PbI_2Cl$ based thin-film perovskite solar cell. *American Journal of Energy Research, 3*(2),19–24.

Wehrenfennig, C., Eperon, G. E., Johnston, M. B., Snaith, H. J., & Herz, L. M. (2013). High Charge Carrier Mobilities and Lifetimes in Organolead Trihalide Perovskites. *Advanced Materials, 26*(10), 1584–1589

Won LS, Kim S, Bae S, Cho K, Chung T, Mundt LE, Lee S, Park S, Park H, Martin CS, Stefan WG, Yohan K, Jun Y, Kang Y, Lee HS, Kim D. (2016) UV degradation and recovery of perovskite solar cells. *Scientific Reports. 6*(38150),1–10.

Yin W.-J., (2014) "Unusual defect physics in CH3NH3PbI3 perovskite solar cell absorber", *Appl. Phys. Lett.,* 104, 063903.

Yifan Z, Rui S, Zhaojian X, Deying L, Hua D, Jiao B, Zhaoxin W, Qihuang G, Rui Z, (2019) perovskitesolar cell towards a lower toxicity: a theoretical study of physical lead reduction strategy. *Science bulletin 64,* 1255-1261.

Zeman M., (2003) Introduction to photovoltaic solar energy. pp. 1–139.

Zhou, H., Chen, Q., Li, G., Luo, S., Song, T., Duan, H. S. Yang, Y. (2014). Interface engineering of highly efficient perovskite solar cells. *Science, 345*(6196), 542–54.

How to cite this paper: Owolabi Joshua Adeyemi, Haruna Ali, Ismaila Musa, Ugbe Raphael Ushiekpan, Bamikole Johnson Akinade, Mohammad Lamido Madugu (2021). Optimization of Lead Base Perovskite Solar Cell with ZnO and CuI as ETM and HTM Using SCAPS-1D. *Malaysian Journal of Applied Sciences, 6*(2), 69-84.